Model Identification of an Unmanned Underwater Vehicle via an Adaptive Technique and Artificial Fiducial Markers

João Britto *†, Diego Cesar *†, Rafael Saback *†, Sascha Arnold †, Christopher Gaudig† and Jan Albiez*†
*Brazilian Institute of Robotics, SENAI CIMATEC, Salvador, Bahia, Brazil, Email: joao.neto@fieb.org.br
†Robotics Innovation Center, DFKI GmbH, Bremen, Germany

***Abstract*—To control any kind of unmanned underwater vehicle (UUV) it is important to know the dynamic model of the system. Creating the model itself is only the first step, the second is identifying the model's parameters. Due to the non-linear and coupled characteristics of UUVs this is a complex and operationally demanding task. Several methods to identify the model parameters have been published in recent years. One of the biggest challenges is providing a data set of the vehicle's true motion, which has not been solved completely. This paper presents and evaluates a new method to identify the motion model parameters of a UUV. The method uses the UUV's pose estimation, the on-board cameras, fiducial markers and an adaptive method to combine the resulting data. The new method is used to parameterize the model of the FlatFish AUV. The paper closes with a comparison of the new method for model identification and the traditional least-squares method using on-board sensors.**

I. Introduction

Knowing the dynamic model of an unmanned underwater vehicle (UUV) is an important requirement for operational tasks such as model-based control, simulation in virtual environments and navigation. Identification of the model's parameters usually is a time-consuming and complex task, since the dynamic of underwater vehicles is non-linear and has coupled characteristics. Several parameter identification techniques for AUVs and remotely operated vehicles (ROVs) were published over the past two decades. In a simple classification, they can be defined as either offline or online techniques, depending on whether they are applied during the system's normal operation. Most of the work focuses on the identification of uncoupled 1-degree-of-freedom (DOF) motion models. However, recent advances have also developed coupled motion model identification.

One commonly used offline technique applied to underwater vehicles is the least-squares method, that has proven its effectiveness in many previous works [1], [2], [3], [4], and also for coupled models [5], [6]. Because of this it is usually employed as a reference in the evaluation of new identification techniques. In the field of online identification techniques, some work has been done using neural networks [7], Kalman filters [8] and adaptive techniques, both for decoupled motion models [9], as for coupled ones [10]. In the context of this work, the adaptive technique presented in [9] has some advantages since it does not require acceleration measurements, it considers a simplified decoupled motion model and its parameters' Lyapunov convergence is assured. Besides that, the experiments using a real vehicle have shown its efficacy.

Usually, parameter identification techniques use on-board sensors in order to collect experimental data to compute the model parameters. Commonly used sensors are a Doppler velocity log (DVL), inertial measurement unit (IMU), fiber-optic gyroscope (FOG), pressure sensor and long and ultra-short baseline acoustic positioning systems (LBL/USBL), enabling the computation of the 6-D vehicle state. Some of those sensors may not be suitable for certain applications, like low-cost or very compact vehicles. On the other hand, being affordable and compact, a camera can provide a real-time pose estimation. For that purpose, a reliable strategy is to use artificial fiducial markers, which are planar markers designed to be easily detected by computer vision systems. They provide a means to estimate the camera's pose in respect to the marker accurately [11].

Since most inspection, survey or research AUVs and ROVs are equipped with a camera, this work shows its relevance by combining the adaptive parameter identification with a pose estimation using fiducial markers in order to obtain a dynamic motion model of the UUV. In [5], an external camera was used to obtain an ROV's motion model, where the vision-based pose estimation was combined with the least-squares technique for the vehicle's parameter identification. [3] used a camera attached to a robot and known visual features located on the bottom of a water tank for vision-based navigation and motion model identification. To the best knowledge of the authors, an on-board camera pose estimation using established markers has not yet been used for model identification purposes, and this solution provides an advantage since it does not depend on the use of an additional camera.

A. Motion Model Parameter Identification

The general dynamic equation of motion used for an underwater vehicle is of the form [12]:

$$M\dot{\upsilon} + C(\upsilon)\upsilon + D(\upsilon)\upsilon + b(\eta) = \tau \tag{1}$$

where M corresponds to the sum of body mass and added mass. C are the Coriolis and centripetal forces due to M.

D is the damping term and it is usually decomposed into linear (D_L) and quadratic (D_Q) terms. b is the buoyancy force and τ are the thruster forces and torques applied to the vehicle. M, C, (D_L) and (D_Q) are $6x6$ matrices while b and τ are $6x1$ vectors.

978-0-933957-43-5 ©2015 MTS

A common approach for simplifying the 6-DOF model consists in considering the added mass constant and neglecting off-diagonal and coupling terms. Those assumptions are made by considering the vehicle to operate at small velocities and to be symmetrical in its three planes. Based on these assumptions, the 1-DOF dynamic equation proposed in [9] is:

$$m_i \dot{\upsilon}_i(t) + d_{Q_i} \upsilon_i(t)|\upsilon_i(t)| + d_{L_i} \upsilon_i(t) + b_i = \tau_i(t), \quad m_i > 0; \quad d_{L_i}, d_{Q_i} > 0 \tag{2}$$

where, for each DOF i, m_i is the total mass, d_{Q_i} and d_{L_i} represent the damping terms, b_i is the buoyancy and τ_i is the control force. Isolating acceleration, (2), becomes

$$\dot{\upsilon}_i(t) = \alpha_i \tau_i(t) + \beta_i \upsilon_i(t)|\upsilon_i(t)| + \mu_i \upsilon_i(t) + \nu_i \tag{3}$$

that can be represented in the vector form

$$\dot{\upsilon}_i(t) = \Phi_i^T f(t)_i \tag{4}$$

where $\Phi_i = [\alpha_i; \ \beta_i; \ \mu_i; \ \nu_i]_{4x1}$ is the vector of the lumped model's parameters and $f(t)_i = [\tau_i(t); \ \upsilon_i(t)|\upsilon_i(t)|; \ \upsilon_i(t); \ 1]$ is the non-linear vector of states and control input.

The least-squares algorithm can be applied using experimental data of 1-DOF vehicle movements and it requires data for $\dot{\upsilon}_i(t)$, $\upsilon_i(t)$ and $\tau_i(t)$.

Considering $\dot{\bar{V}}_i = [\dot{\upsilon}_i(t_1) \cdots \dot{\upsilon}_i(t_n)]_{1xn}$ and $\bar{F}_i = [f_i(t_1) \cdots f_i(t_n)]_{4xn}$ being data of n samples, then (4) leads to

$$\dot{\bar{V}}_i = \Phi_i^T \bar{F}_i \tag{5}$$

which can be solved with the standard pseudo-inverse, in case $\bar{F}_i$ is full-rank:

$$\Phi_i = (\dot{\bar{V}}_i \bar{F}_i^T (\bar{F}_i \bar{F}_i^T)^{-1})^T \tag{6}$$

For the adaptive parameter identification proposed in [9], given (4), an adaptive estimator is given by

$$\dot{\hat{\upsilon}}(t) = a_m \Delta\upsilon(t) + \hat{\Phi}^T \hat{f}(t) \tag{7}$$

where $\hat{f}(t) = [\tau(t); \ \hat{\upsilon}(t)|\hat{\upsilon}(t)|; \ \hat{\upsilon}(t); \ 1]_{4x1}$, $\hat{\upsilon}(t)$ representing an estimated velocity, $\hat{\Phi}(t)$ are the estimated lumped parameters Φ and $a_m < 0$ is a gain. The terms $\Delta\upsilon(t) = \hat{\upsilon}(t) - \upsilon(t)$ and $\Delta\dot{\Phi}(t) = \dot{\hat{\Phi}}(t); \dot{\Phi} = 0$ represent coordinate errors. The parameter update law is defined as

$$\Delta\dot{\Phi}(t) = -\Lambda \Delta\upsilon(t) \hat{f}(t) \tag{8}$$

where $\Lambda = diag[\lambda_i]$, for $i = 1 \cdots 4$, with $\lambda_i > 0$.

A complete analysis of the adaptive identifier and its proof of convergence in the sense of Lyapunov can be found in [9]. A generic overview of the data flow in the adaptive method is shown in Fig. 1.

B. Camera pose estimation

The process of estimating the camera's pose with respect to an object is desired in many applications such as robot navigation and augmented reality. In the case of an online pose estimation, where a new pose is calculated for each frame using the information provided by a single image, the intrinsic parameters of the camera and a previous knowledge of the scene are required.

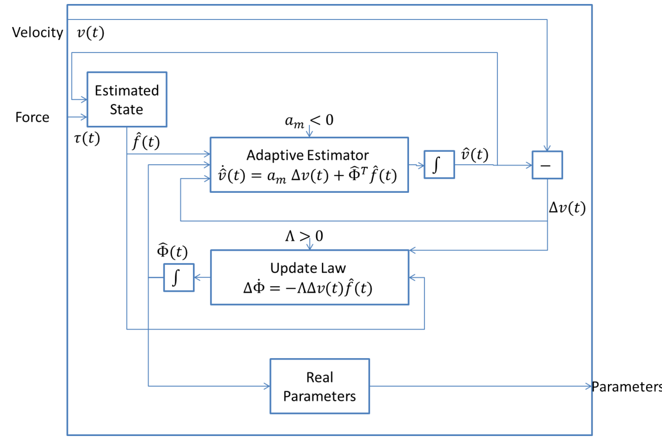

Fig. 1: Adaptive model data flow

For the pose computation, four co-planar (but non-collinear) points on the image plane need to be extracted, whose displacement in world coordinates are known [13]. In that context, when it is possible to modify the environment, fiducial markers provide large advantages over the detection of natural features [14], because they are designed to be easily detected by computer systems, robust to false-positives and false-negatives and achieve a high detection rate [11]. This way, the use of fiducial markers allows to quickly and reliably extract the four corners' coordinates on the image plane and correlate them with the known dimensions of the real object. This correlation is performed using a Perspective-n-Point (PnP) approach that computes the camera pose in relation to the planar marker.

Among the different types of fiducial markers, [14] has compared the performance of three widely used open-source marker systems in underwater environments. This work has suggested that the AprilTags marker system outperforms the other tested marker systems under different turbidity and lighting levels, being detectable at larger distances and angles.

II. Experiment Procedures

A. Experiment Setup

The experiments were conducted in a 23m x 19m x 8m saltwater test basin at the Maritime Exploration Hall[1] of the DFKI Robotics Innovation Center (RIC). Although the turbidity level of the water was not verified, no significant turbidity was perceived. A new underwater vehicle named FlatFish, developed by RIC and the Brazilian Institute of Robotics (BIR), was used for the experiments. The robot has a mass of 274kg and its dimensions are 2.10m x 1.02m x 0.5m (LxWxH) [15].

Data from on-board sensors (DVL, IMU-FOG and pressure sensor) was fused using an already existing pose estimator component in the Rock[2] framework. The vehicle's velocities provided by the module were treated as true values.

[1] http://robotik.dfki-bremen.de/en/research/research-facilities/maritime-exploration-hall.html

[2] Robot Construction Kit: http://www.rock-robotics.org

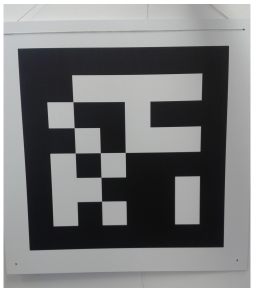

Fig. 2: ApriTag marker

The on-board forward-looking camera features a resolution of 2040px x 2040px (Basler acA2040-25gm). One AprilTag marker (0.4m x 0.4m), shown in Fig. 2, was placed on the tank's wall at an arbitrary depth. As no significant disturbance was perceived, the marker was considered to remain at a constant position during the experiment. The marker type was chosen according to [14]. It was used for pose estimation using the camera.The size of the marker, the quality of the camera and the clarity of the water allow the AprilTag algorithm to detect the marker even from the tank's opposite wall.

The vehicle is actuated by six Enitech thrusters, which receive as input a setpoint rotational speed, in Hz (i.e. revolutions per second). Experiments performed by the manufacturer show the relation of thrust and angular propeller velocity, which matches the common thruster model used in [16]:

$$Thruster = C_t \Omega |\Omega| \tag{9}$$

B. Methodology

A control chain based on PID controllers was already implemented in Rock and was used to perform the experiments. As the vehicle is actively controlled in five DOF (surge, sway, heave, yaw and pitch), the control chain was used to keep the position in four of the DOF while the vehicle could perform an oscillatory movement along the remaining DOF.

For this work, surge, yaw and heave motions were performed individually. The experiments were driven by either a closed-loop control of one DOF or an open-loop command to the thrusters while the motion was monitored. Details of the experiments are shown in Table I.

TABLE I: Experiment Inputs

DOF	Input	Sine Amplitude	Sine Frequency
Surge	Open-loop body frame	52.9 [N]	0.3 [rad/s]
Heave	Closed-loop world frame	1 [m]	0.3 [rad/s]
Yaw	Closed-loop world frame	0.3 [rad]	0.3 [rad/s]

The robot was initially placed in the center of the tank, facing the marker, see Fig. 3. The test duration was around 5 minutes for each DOF experiment. Although the robot is not symmetrical regarding the y-z plane and x-y plane, for experimental simplicity the movements and models identified did not take that into account.

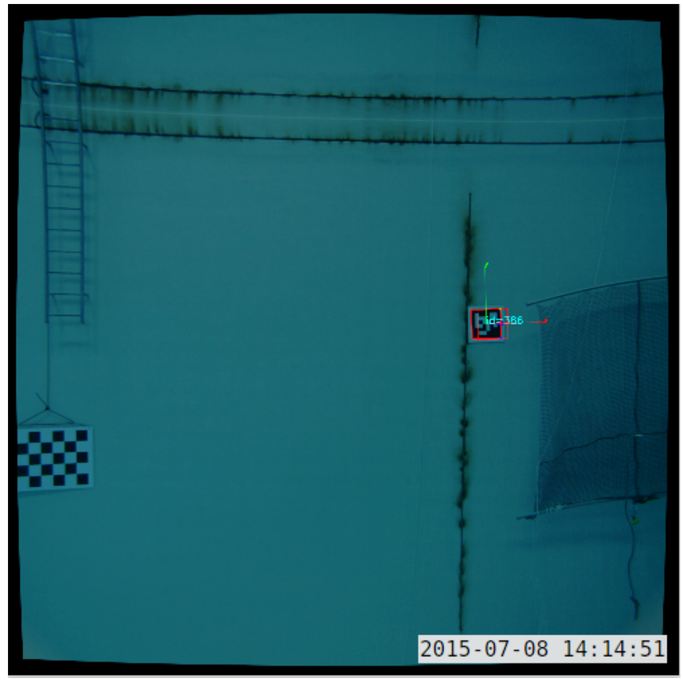

Fig. 3: View from on-board camera with detected marker

Experiment data from the pose estimator (fused underwater sensors), the camera pose (pose computed by the AprilTag detector) and the control signal sent to the thrusters was logged, each sample with a timestamp for data analysis. The adaptive method proposed by [9] was implemented within the Rock framework, receiving as input velocity and force data for a specified DOF.

The least-squares method was employed using singular value decomposition (SVD). The C++ library is available in [17]. A Savitzky-Golay filter algorithm [18] was used for computing velocities from the camera poses and also accelerations from the pose estimator and camera poses.

A general overview of the data flow and components used is shown in Fig. 4. Four model parameters were estimated for each DOF using a combination of two different identification techniques (adaptive and least-squares) and two sensing methods (pose estimator and camera pose).

In order to evaluate the quality of the identified models, a mean absolute error (MAE) was computed comparing the velocity of the model with the measured velocity. The MAE is given by:

$$mae = mean(|v_{model} - v_{measured}|) \tag{10}$$

Another metric was established in order to measure the quality of the model found. The proposed metric is called normalized mean absolute error (NMAE), given by:

$$nmae = \frac{mean(|v_{model} - v_{measured}|)}{mean(|v_{measured}|)} \tag{11}$$

The adaptive method was implemented using Euler integration.

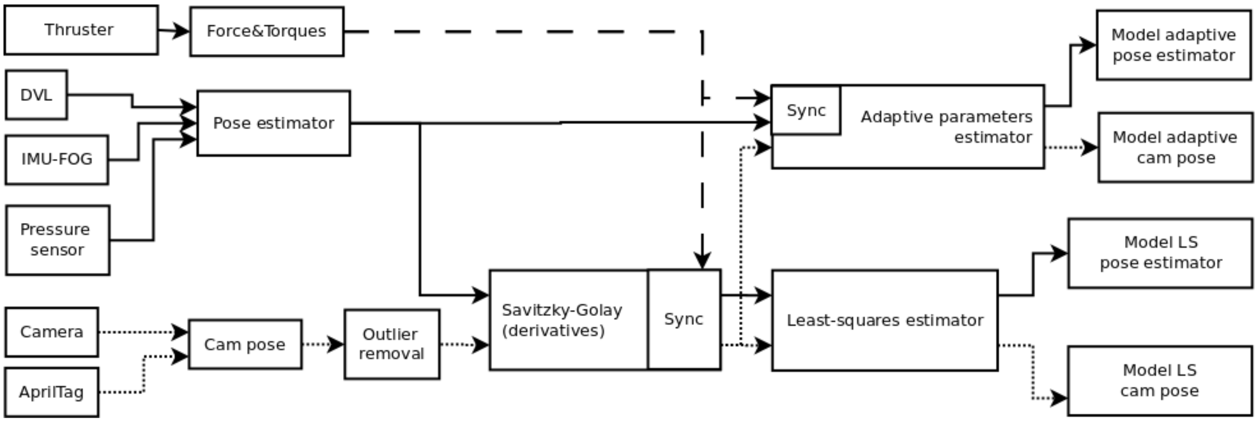

Fig. 4: Data flow and components used for motion model parameter identification

TABLE II: Parameter Comparison

DOF	Model	Inertia	Q. Damping	L. Damping	Buoyancy	MAE	NMAE
Surge	Adaptive pose estimator	890.28 [kg]	6.78 [kg/m]	38.82 [kg/s]	-0.97 [N]	0.01588 [m/s]	0.1373
	Adaptive cam pose	909.8 [kg]	10.85 [kg/m]	61.01 [kg/s]	-0.14 [N]	0.01684 [m/s]	0.1456
	LS pose estimator	851.05 [kg]	8.62 [kg/m]	39.57 [kg/s]	-0.81 [N]	0.01527 [m/s]	0.1321
	LS cam pose	1011.7 [kg]	55.68 [kg/m]	49.92 [kg/s]	-0.91 [N]	0.01885 [m/s]	0.1630
Heave	Adaptive pose estimator	1521.45 [kg]	2.24 [kg/m]	31.40 [kg/s]	-12.67 [N]	0.01610 [m/s]	0.3293
	Adaptive cam pose	5400 [kg]	1.6 [kg/m]	28 [kg/s]	-11.4 [N]	0.03527 [m/s]	0.7210
	LS pose estimator	1511.53 [kg]	1911.21 [kg/m]	-70.29 [kg/s]	-12.42 [N]	0.006935 [m/s]	0.1417
	LS cam pose	3206.85 [kg]	-754.85 [kg/m]	101.76 [kg/s]	-11.45 [N]	0.02465 [m/s]	0.5039
Yaw	Adaptive pose estimator	317.21 [kg*m^2/rad]	334.41 [kg*m^2]	1.75 [kg*m^2/(rad*s)]	0.08 [N*m]	0.0109 [rad/s]	0.2686
	Adaptive cam pose	343.36 [kg*m^2/rad]	174.91 [kg*m^2]	11.78 [kg*m^2/(rad*s)]	-0.25 [N*m]	0.01457 [rad/s]	0.3564
	LS pose estimator	301.60 [kg*m^2/rad]	279.39 [kg*m^2]	26.92 [kg*m^2/(rad*s)]	-0.0909 [N*m]	0.01128 [rad/s]	0.2763
	LS cam pose	317.59 [kg*m^2/rad]	154.28 [kg*m^2]	10.29 [kg*m^2/(rad*s)]	-0.072 [N*m]	0.01363 [rad/s]	0.3337

III. RESULTS AND DISCUSSION

Table II shows the model's parameters and performance.

According to [9], the buoyancy term for DOFs other than Heave can be interpreted as small offset errors of the thruster calibration.

An analysis of the errors calculated shows that the least-squares model using the pose estimator data has better performance in surge and heave DOFs followed by the adaptive model using the same source of data. For the yaw DOF, the adaptive pose estimator model performed better, followed by the least-squares pose estimator model. Underwater sensors provide a direct and consistent measurement of velocities and a first derivative for the acceleration estimation using a Savitzky-Golay showed to be reliable, although errors in measurement impact the quality of derivatives.

The models computed using the visual pose performed not as well as models with fused underwater sensors. An analysis of both identification method with camera pose shows that non discrepant results were found between them in surge and yaw, although the least square method performed better in two of three DOF (heave and yaw). It was observed from the experiment that the camera pose provides an unsatisfactory heave position, while it supplies reliable surge and yaw information. One possible explanation is that the amplitude of the motion for the heave experiment was not as desired.

Fig 5 shows the response of each identified model compared with the measured velocity. The parameters estimated for the four models have the same order of magnitude. Knowing the dry mass of the vehicle (274 kg) and its dimensions, an inertia of around 900 kg in surge, 1510 kg in heave and 317 kg*m^2/rad in yaw seems reasonable. Comparing this with the result of [9], where a total mass for the surge direction of 290 kg, 2646 kg for heave and 132 kg*m^2/rad for yaw was found for an open-frame vehicle with a dry mass of 140 kg, the result of this work can be considered acceptable.

Inconclusive results were found regarding which identification techniques provide the most trustworthy model parameters. Both methods provide good results. For the model identification using visual pose data from the AprilTag marker, the decoupled motion model parameters for the surge and yaw DOFs present good results, even though not as good as the pose estimator case. However, inconclusive results for the heave DOF using camera poses were observed.

The authors are aware that cross-validation experiments and more tests for the heave DOF need to be performed. Although this do not invalidate the obtained results they are topics for future works.

The pros and cons observed from the different techniques

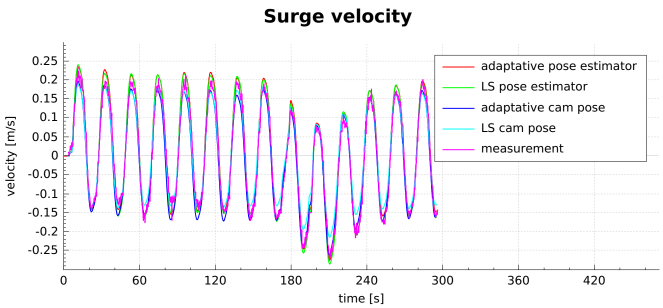

(a)

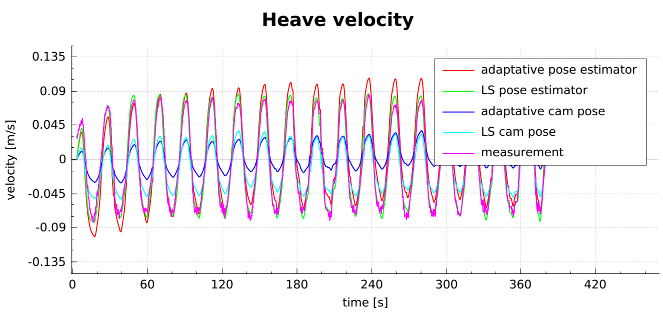

(b)

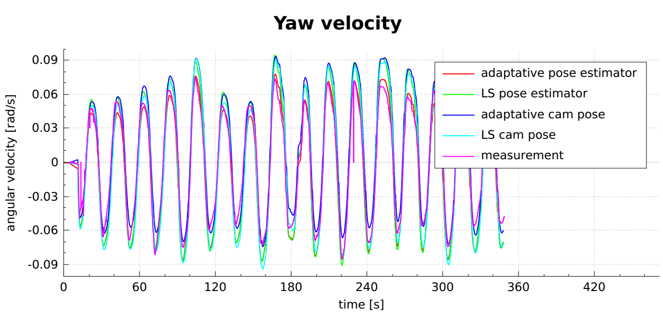

(c)

Fig. 5: Comparison of each model's response with the measured velocity. (a) Surge direction. (b) Heave direction. (c) Yaw direction.

are described. The adaptive parameter identification proved to be reliable in estimating constant value parameters. The fact that it can be implemented online is also an advantage, especially for reconfigurable vehicles. Nevertheless, the amount of gain values to be tuned empirically is a disadvantage and may turn into a time-consuming task. The least-squares method gives a direct result for a parameter, even though it does not provide an online identification and the indirect acceleration data may be questionable, especially through a second derivative. The use of an on-board camera and an AprilTag marker with a Savitzky-Golay filter have been shown to be satisfactory in estimating model parameters, especially for the surge and yaw DOFs. An online implementation using the adaptive method is possible, although a delay of the identification may be introduced depending on filter and derivative properties. This technique may be of interest for underwater vehicles equipped with an on-board camera that lack high-priced underwater sensors.

IV. Conclusion

This paper evaluates the performance of motion model parameter identification for unmanned underwater vehicles via a combination of two parameter identification techniques (adaptive identifier [9] and least-squares method) and two sources of pose data (fusion of underwater sensors and visual poses using an AprilTag marker), combined in order to provide four uncoupled single-DOF motion models in surge, yaw and heave. A brief overview of motion model parameter identification methods was presented here. A summary of the motion model, the adaptive and least-squares parameter identifiers, as well as the visual pose using an AprilTag detector was given.

Among the four models identified for each DOF and the metrics used, the least-squares method performed slightly better than the adaptive identifier. Regarding the source of pose data, underwater sensor data provided a better estimation than visual poses. Nevertheless, the motion model identified via visual poses still provides good parameters for the surge and yaw DOFs. The visual poses for the heave DOF were not reliable during the experiments and more tests need to be performed in order to obtain conclusive results.

This work concludes that the visual pose estimation for model identification appears as a good alternative for underwater vehicles that contain an on-board camera but are not equipped with costly underwater sensors for velocity measurements. With a motion model identified, advancements in model-based control, simulation in virtual environments and for navigation purposes can be achieved.

A. Future Work

A decoupled single-DOF motion model was considered in this work. As a next step, the dynamic reliability of the motion model during the vehicle's operation and the necessity of applying a coupled motion model will be analyzed. A pose given by multiple visual markers will be considered and compared with underwater sensors. The computational effort and complexity of implementation of a coupled motion model identification will be considered.

Acknowledgment

The work presented in this paper was done in cooperation with the FlatFish project, an ongoing research and development program of BG Group Brazil. It is funded by the Brazilian government via the Agência Nacional do Petróleo, Gás Natural e Biocombustíveis (ANP) and, due to its highly innovative nature, co-funded by the EMPRAPII (Empresa Brasileira de Pesquisa e Inovação Industrial) program.

The authors would like to thank all colleagues involved at SENAI and DFKI for their support.

References

[1] M. Caccia, G. Indiveri, and G. Veruggio, "Modeling and identification of open-frame variable configuration unmanned underwater vehicles," *Oceanic Engineering, IEEE Journal of*, vol. 25, no. 2, pp. 227–240, April 2000.

[2] S. Natarajan, C. Gaudig, and M. Hildebrandt, "Offline experimental parameter identification using on-board sensors for an autonomous underwater vehicle," in *Oceans, 2012*, Oct 2012, pp. 1–8.

[3] P. Ridao, A. Tiano, A. El-Fakdi, M. Carreras, and A. Zirilli, "On the identification of non-linear models of unmanned underwater vehicles," *Control Engineering Practice*, vol. 12, no. 12, pp. 1483 – 1499, 2004, guidance and control of underwater vehicles. [Online]. Available: http://www.sciencedirect.com/science/article/pii/S0967066104000152

[4] A. Alessandri, M. Caccia, G. Indiveri, and G. Veruggio, "Application of ls and ekf techniques to the identification of underwater vehicles," in *Control Applications, 1998. Proceedings of the 1998 IEEE International Conference on*, vol. 2, Sep 1998, pp. 1084–1088 vol.2.

[5] N. Miskovic, Z. Vukic, and M. Barisic, "Identification of coupled mathematical models for underwater vehicles," in *OCEANS 2007 - Europe*, June 2007, pp. 1–6.

[6] S. Martin and L. Whitcomb, "Preliminary experiments in comparative experimental identification of six degree-of-freedom coupled dynamic plant models for underwater robot vehicles," in *Robotics and Automation (ICRA), 2013 IEEE International Conference on*, May 2013, pp. 2962–2969.

[7] P. W. van de Ven, T. A. Johansen, A. J. Sørensen, C. Flanagan, and D. Toal, "Neural network augmented identification of underwater vehicle models," *Control Engineering Practice*, vol. 15, no. 6, pp. 715 – 725, 2007, special Section on Control Applications in Marine SystemsCAMS2004Control Applications in Marine Systems. [Online]. Available: http://www.sciencedirect.com/science/article/pii/S0967066105002467

[8] G. Karras, S. Loizou, and K. Kyriakopoulos, "On-line state and parameter estimation of an under-actuated underwater vehicle using a modified dual unscented kalman filter," in *Intelligent Robots and Systems (IROS), 2010 IEEE/RSJ International Conference on*, Oct 2010, pp. 4868–4873.

[9] D. Smallwood and L. Whitcomb, "Adaptive identification of dynamically positioned underwater robotic vehicles," *Control Systems Technology, IEEE Transactions on*, vol. 11, no. 4, pp. 505–515, July 2003.

[10] C. McFarland and L. Whitcomb, "Comparative experimental evaluation of a new adaptive identifier for underwater vehicles," in *Robotics and Automation (ICRA), 2013 IEEE International Conference on*, May 2013, pp. 4614–4620.

[11] M. Fiala, "Designing highly reliable fiducial markers," *Pattern Analysis and Machine Intelligence, IEEE Transactions on*, vol. 32, no. 7, pp. 1317–1324, July 2010.

[12] T. I. Fossen, *Guidance and control of ocean vehicles*. John Wiley & Sons Inc, 1994.

[13] G. Schweighofer and A. Pinz, "Robust pose estimation from a planar target," *Pattern Analysis and Machine Intelligence, IEEE Transactions on*, vol. 28, no. 12, pp. 2024–2030, Dec 2006.

[14] D. Cesar, C. Gaudig, M. Fritsche, M. Reis, and F. Kirchner, "An evaluation of artificial fiducial markers in underwater environments," in *OCEANS 15 - Genova*. IEEE, 2015.

[15] J. Albiez, S. Joyeux, C. Gaudig, J. Hilljegerdes, S. Kroffke, C. Schoo, S. Arnold, G. Mimoso, P. Alcantara, R. Saback, J. Britto, D. Cesar, G. Neves, T. Watanabe, P. Merz Paranhos, M. Reis, and F. Kirchner, "FlatFish – a compact subsea-resident inspection auv," in *Proceedings of the MTS/IEEE OCEANS 2015*, Washington DC, USA, Oct 2015, pp. 1–8.

[16] D. Yoerger, J. Cooke, and J.-J. Slotine, "The influence of thruster dynamics on underwater vehicle behavior and their incorporation into control system design," *Oceanic Engineering, IEEE Journal of*, vol. 15, no. 3, pp. 167–178, Jul 1990.

[17] G. Guennebaud, B. Jacob *et al.*, "Eigen v3," http://eigen.tuxfamily.org, 2010.

[18] P. A. Gorry, "General least-squares smoothing and differentiation by the convolution (savitzky-golay) method," *Analytical Chemistry*, vol. 62, no. 6, pp. 570–573, 1990. [Online]. Available: http://dx.doi.org/10.1021/ac00205a007